



Universiteit
Leiden
The Netherlands

Gochlear implants from model to patients

Briaire, J.J.

Citation

Briaire, J. J. (2008, November 11). *Gochlear implants from model to patients*. Retrieved from <https://hdl.handle.net/1887/13251>

Version: Corrected Publisher's Version

License: [Licence agreement concerning inclusion of doctoral thesis in the Institutional Repository of the University of Leiden](#)

Downloaded from: <https://hdl.handle.net/1887/13251>

Note: To cite this publication please use the final published version (if applicable).

Chapter 5

The Importance of Human Cochlear Anatomy for the Results with Modiolus Hugging Multi-Channel Cochlear Implants

Johan H.M. Frijns, Jeroen J. Briaire and Jan J. Grote
Otology and Neurotology (2001), 22, 340-349

Abstract

Hypothesis: The fact that the anatomy of the basal turn of the human cochlea, especially, is essentially different from that of other species is likely to influence the outcome of cochlear implantation.

Background: Multichannel cochlear implants give better speech understanding than single-channel devices. They are intended to make use of the tonotopic organization of the cochlea by selectively stimulating subpopulations of the auditory nerve. At higher stimulus levels and with monopolar stimulation, excitation of nerve fibers from other turns may interfere with this concept, especially with modiolus-hugging electrodes.

Methods: A three-dimensional spiraling computer model of the human cochlea, based on histological data, was used to test the spatial selectivity and the dynamic range before cross-turn stimulation takes place for the Clarion HiFocus implant with and without a positioner. The results were compared with a similar model of the guinea pig cochlea.

Results: In humans (in contrast to the guinea pig), a well-designed modiolus-hugging electrode yielded reduced current thresholds and high spatial selectivity without reduction of the useful dynamic range. The apical turn of the human cochlea, however, is largely comparable in this respect with the guinea pig cochlea, where cross-turn stimulation reduces the dynamic range substantially.

Conclusion: The clinical success of cochlear implantation in humans and the favorable results with modiolus-hugging devices depend on the anatomy of the human cochlea.

5.1 Introduction

The successful application of multichannel devices is the main factor contributing to the breakthrough in performance by cochlear prostheses for the totally deaf during the last decade. In contrast to single-channel designs, multichannel cochlear implants take advantage of the tonotopic organization in the cochlea by trying to stimulate localized subpopulations of nerve fibers with each electrode or electrode combination in the electrode array. The spatial selectivity thus achieved is the electrical counterpart of the mechanical tuning present in the normal cochlea. The continuous interleaved sampling strategy (Wilson et al., 1991) and various strategies used with the Nucleus (Cochlear Corp., Melbourne, Australia) device, which that use sequential, nonsimultaneous stimulation of the electrodes, have thereby proved important in avoiding the problems associated with direct electrical interaction between electrodes. There is still, however, a mismatch between the small number of independent input channels and the thousands of surviving nerve fibers to be stimulated. Therefore, the need is perceived for further refinement of the electrode array to include many more electrodes to stimulate small groups of auditory nerve fibers (Clark, 1999). For this to be feasible, even with nonsimultaneous stimulation, the regions of the cochlea excited by the various electrodes must not overlap excessively, i.e., the electrodes must have sufficient spatial selectivity. Some recent experiments suggest, however, that changes in the peak or edge of the excitation pattern are more important than the relative amount of nonoverlap of the excitation areas from the two electrodes, at least for discrimination tasks (McKay et al., 1999).

In previous articles, we addressed the question of neural excitation and spatial selectivity with cochlear implants, using a computational model of the electrically implanted guinea pig cochlea (Frijns et al., 1995; Frijns et al., 1996a). As validation, we compared the results with experimental evoked auditory brainstem responses (Shepherd et al., 1993) and single-fiber (van den Honert and Stypulkowski, 1987) data in the literature and found a good agreement with the model predictions. It was shown that both the excitation threshold and the spatial selectivity depend strongly upon on the exact position of the stimulating current sources in the scala tympani. Moreover, the simulations, including more recent ones with a truly spiraling cochlear model (Frijns et al., 2000a; Briare and Frijns, 2000b), demonstrated that the upper range of useful stimulus levels is limited by so-called ectopic or cross-turn stimulation rather than by current spread along the scala tympani, as is widely assumed. This

cross-turn stimulation occurs when the stimulating electrodes excite the modiolar part of the auditory nerve fibers originating in more apical turns, i.e., those fibers physiologically associated with lower frequencies. Therefore, this phenomenon is expected to cause substantially different percepts at higher stimulation levels.

Several advantages are associated with a reduction of the current threshold. First, this increases the safety margin before the electrochemical processes at the electrodes can produce potentially noxious products. Because these processes are primarily controlled by the current density at the electrode surface (Brummer and Turner, 1977), it is necessary to limit the stimulating currents if larger numbers of smaller electrode contacts are to be used in future cochlear implants. Also, total power consumption, important with behind-the-ear or fully implantable devices (Maniglia et al., 1999), is beneficially affected by reducing stimulus levels. With currently available cochlear implants, many patients are programmed in monopolar stimulation modes, because this leads not only to lower thresholds but also to saturation at lower stimulus levels than, for example, bipolar or quadripolar configurations (Chatterjee, 1999). To increase selectivity with such broadly spreading current sources, several methods have been proposed to move the electrode array toward the modiolus (Gstoettner et al., 1999; Kuzma and Balkany, 1999; Aschendorff et al., 1999), i.e., closer to the fibers to be stimulated. This modiolus-hugging principle is also expected to yield further reduced threshold levels and will lead to a deeper insertion if the same length of the electrode carrier is bent along the modiolar rather than the outer wall of the scala tympani.

If however, this modiolus-hugging principle is viewed in the light of the results obtained in our simulations with the guinea pig model, it is doubtful whether it will be as beneficial as might initially be thought. Moving the current source toward the modiolus means not only that it approaches the fibers it should stimulate, but that it will also come closer to the modiolar parts of the fibers from more apical turns. The risk of early cross-turn stimulation is therefore increased, and the overall gain associated with modiolus-hugging depends on the recruitment characteristics of the different fiber populations. These recruitment characteristics are expected to depend on the relative location of the fibers and the stimulating electrodes. Consequently, it is conceivable that the answer to the question whether approaching the modiolus with the electrode array is favorable may depend on the species-specific anatomy of the cochlea. Cochlear anatomy differs between humans and nonhuman primates and also between humans and most other species, including guinea pigs and cats, in ways quite apart from size (Fig. 5.1). In humans the second and third turns

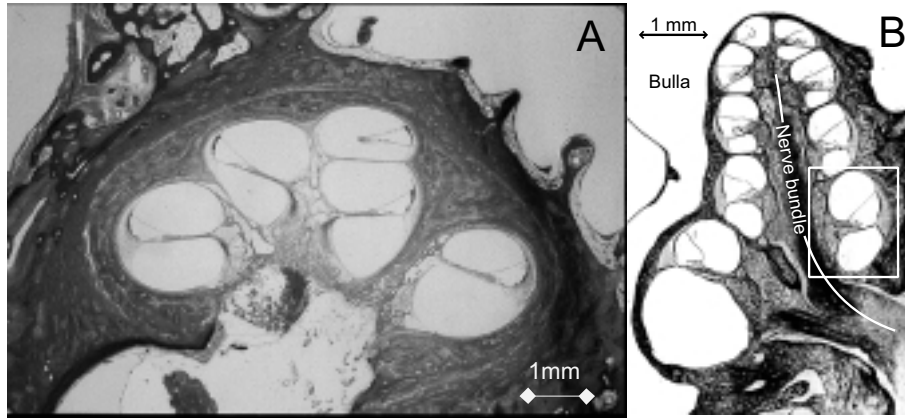


*Figure 5.1: **A:** Midmodiolar cross-section of the human cochlea, showing the large distance between the basal turn and the central modiolar axis. All turns have a specific shape of the three scalae and the apical turns are more or less embedded in the basal turn (Courtesy of Dr F. Linthicum, House Ear Institute). The white bar with diamond-shaped endings has a length of 1 mm and indicates the magnification. **B:** A similar cross-section through the guinea pig cochlea, in which the anatomy of all turns, including their relative distance to the modiulus, is grossly equal apart from a scaling factor. The much smaller size of the guinea pig cochlea is illustrated by the scaling bar in the upper left corner. The white rectangle indicates the turn to which the basic slice is fitted, which is used for the construction of the model.*

are more or less embedded in the basal one, and each turn has its own shape, whereas in the guinea pig all turns are stacked on top of one another and are almost uniformly shaped.

This study addresses the role the species-specific anatomy of the cochlea plays as a determinant of the spatial selectivity and dynamic range attainable with multichannel cochlear implants. For this purpose, fully three-dimensional computer models of the human and the guinea pig cochlea, implanted with clinically relevant macroelectrodes in lateral and modiulus-hugging positions, are compared. The results are discussed in the light of currently available and future electrode geometries.

5.2 Materials and Methods

A computational model of the implanted cochlea was used, which was developed to provide more insight into the fundamentals of functional electrical stimulation of the auditory nerve. The conceptual framework behind this two-step model is as follows: The speech processor delivers the stimulus current via the electrode system, which induces a potential field in the cochlea. This potential field, as computed by the volume conduction model, forms the input of the nerve fiber model that predicts which auditory nerve fibers will be excited. The information conveyed to the brain is characterized by the number, location and firing pattern of these fibers, the model's output. This method has been used successfully before (Frijns et al., 1995; Frijns et al., 1996a; Frijns et al., 2000a; Briaire and Frijns, 2000b), and here we describe only the essentials and the newly introduced methodologic aspects.

5.2.1 Three-dimensional volume conduction model of the human and guinea pig cochlea

The calculation of the potential distribution induced by the currents on the stimulating electrodes is especially intricate in the case of cochlear implants because of the complex geometry of both the inner ear and the electrodes. The boundary element method (BEM) with quadratic interpolation functions for the surface and the potential (Frijns et al., 2000b) was used to solve this problem, as was done in our previous studies. The cochlea is considered to be purely resistive, and capacitive effects (e.g., at the electrode-fluid interface) were not included, because measurements have shown that this assumption is valid for frequencies up to 100 kHz (F. Spelman, personal communication). The conductivity parameters for the various media were those used in our previous studies. The BEM requires discretization of the boundaries between media of different conductivity rather than subdivision of the media themselves. It combines relative ease of mesh generation with the opportunity to deal easily with multielectrode arrays (Briaire and Frijns, 2000a).

The model representations of the human and guinea pig cochlea are based on the histological cross-sections shown in Figure 5.1^A and Figure 5.1^B, respectively. The resulting human mesh has a two and three-quarters turn and is defined by 4,476 surface elements (Fig. 5.2^A). Figure 5.2^B shows how closely the midmodiolar cross-section of this mesh matches the histological slide of Figure 5.1^A. In the model, as in vivo, the higher cochlear turns are more or

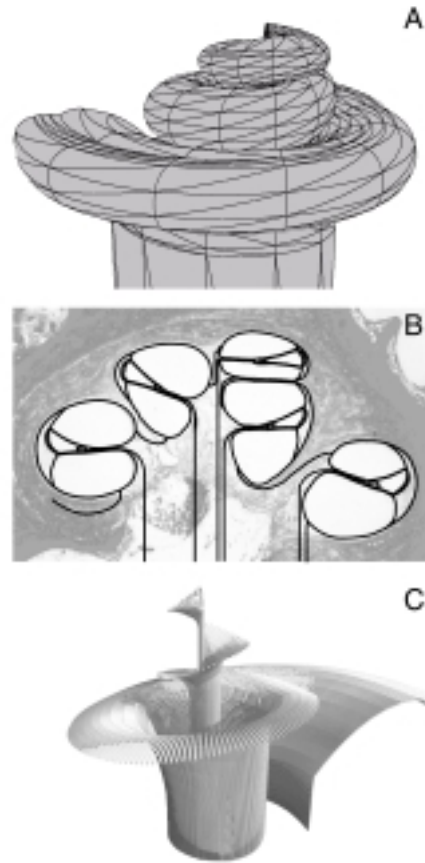
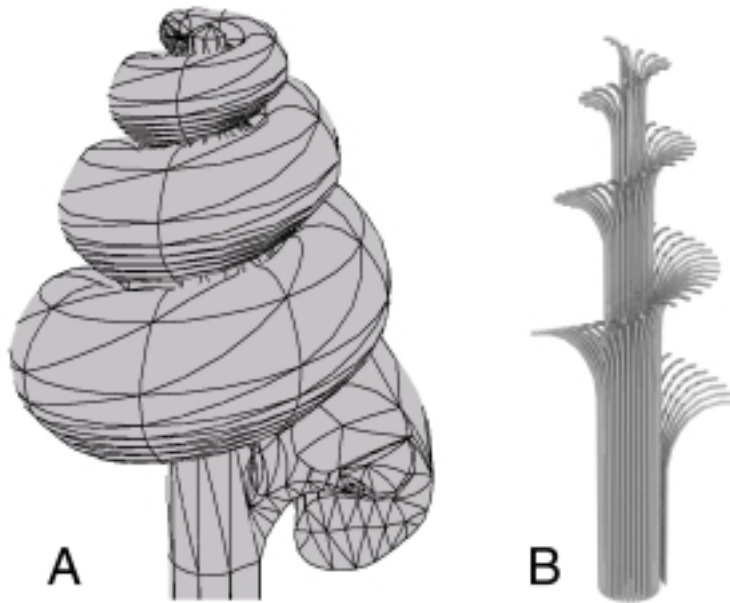


Figure 5.2: A: The boundary element mesh with curved triangular surface elements of the human cochlea as used in the computations. It was constructed on the basis of the histological cross-section of Figure 1A. B: The equivalent midmodiolar cross-section of the human cochlea mesh superimposed upon the histological slice of Figure 1A. The solid lines in the modiolus, exiting the osseous spiral lamina, indicate the course of the nerve fibers. C: Location of the primary auditory nerve fibers in the human cochlea model.



*Figure 5.3: **A:** The boundary element method mesh of the guinea pig cochlea as used in the computations **B:** Location of the primary auditory nerve fibers in the guinea pig cochlea model.*

less embedded in the basal one. Figure 5.2^C shows the spatial distribution of the modeled nerve fibers, which are distributed equidistantly along the basilar membrane with a spacing of approximately $115 \mu\text{m}$ (the unmyelinated terminals of the fibers [see Fig. 5.5] are spaced at $100 \mu\text{m}$). This means that each of the 299 nerve fibers in the simulations represents approximately 100 actual nerve fibers.

Similarly, Figure 5.3 shows the mesh (A) and the fiber distribution (B) in the guinea pig model. This model is somewhat more simplified than the human model, because it was constructed by scaling, and a combination of translation and rotation of a single slice fitted to the boxed part of the histological cross-section as shown in Figure 5.1^B. The details of this procedure, including the anatomically based scaling function, have been published elsewhere (Briaire and Frijns, 2000a). Therefore, the model is slightly limited in its description of

the hook region, but nevertheless it closely resembles the in vivo situation. It has three and a half cochlear turns and includes 405 nerve fibers, with their peripheral endings spaced uniformly every $40 \mu\text{m}$. The most striking difference between this guinea pig model and the human counterpart is the fact that the cochlear turns are stacked on top of one another and that the nerve fibers of all turns, including the basal one, are rather closely packed in the modiolus.

In the human, as well as in the guinea pig, each position in the cochlea is referred to in terms of its rotational position Υ , defined as the number of turns between that position and the basal end of the cochlea. This implies that the rotational position of the apex of the human cochlea is 2.75, whereas it is 3.5 in the guinea pig.

5.2.2 Simulated electrode configurations

In our previously published studies, we used bipolar point current sources rather than realistically shaped (banded) intracochlear electrode arrays. This simplification was dictated by the fact that at that time our software did not allow us to perform calculations with the large meshes that are necessary to include sufficient detail in these electrodes and to achieve the numerical accuracy required for adequately calculating neural responses.

In this study, however, we were interested in the effect of modern modiolus-hugging electrodes, like the Clarion HiFocus device, which have their electrode contacts at the modiolar side of an insulating carrier. This carrier impedes the current flow in the lateral direction, and as expected, this is reflected in the potential distribution in the neural compartment of the cochlea. Therefore, it was necessary to include realistic representations of the electrodes under study, at the cost of increasing the numerical effort involved in the calculations.

Figure 5.4 shows the model representation of the Clarion HiFocus electrode as used in the present study. The human model has 16 rectangular electrode contacts of $0.4 \times 0.5 \text{ mm}$, regularly spaced at 1.1 mm , at the medial side of a Silastic carrier. This slightly tapered carrier has small bulbs medially between the electrode contacts, preventing the electrode surfaces themselves from coming into direct contact with the modiolus. The mesh for this electrode array is defined by 1,678 triangles, adding to a total of 11,483 equations and unknowns to be solved for a solution for this electrode in the human cochlea. The conductivity of the carrier was defined as $10^{-5} (\Omega \cdot \text{m})^{-1}$ and that of the electrode contact as $100 (\Omega \cdot \text{m})^{-1}$. This is an empirical tradeoff between using the actual conductivities (0 and $\pm 10^7 (\Omega \cdot \text{m})^{-1}$ respectively) and avoiding the

numerical errors inherent in the use of large conductivity differences between neighboring media with the BEM. In this way, the conductor is approximately two decades more conductive than the surrounding perilymph, and the insulator is roughly three decades less conductive than the membranes surrounding the scala media.

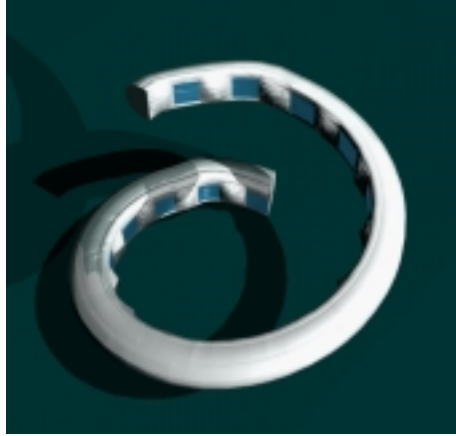


Figure 5.4: Model representation of the new Clarion HiFocus electrode, which has 16 rectangular surface contacts, located at the modiolar side of a silastic carrier. It is intended to be displaced to the modiolar wall of the scala tympani by a positioner, which is introduced separately along the outer curvature. The size of the contacts is 0.4×0.5 mm for the human and 0.18×0.23 mm for the guinea pig model.)

If this electrode is inserted along the outer wall into the scala tympani of the human cochlea model (insertion depth 23.7 mm = 1.03 turn), it is referred to as human lateral. The situation is referred to as human medial if the electrode is inserted alongside the modiolar wall (to a maximum depth of $\Upsilon=1.48$), together with a model replica of the so-called positioner, which has a medial concavity in which the electrode fits neatly. In fact, we fused the meshes of this Silastic strip and the electrode before starting the simulations to avoid unnecessary computations and numerical errors. The corresponding situations in the guinea pig are referred to as GP lateral and GP medial, respectively.

Because the guinea pig cochlea is much smaller than the human one, we downsized the guinea pig electrode and positioner in such a way that they fit into the scala tympani in a similar way as in the human situation. The electrode

contacts were 0.18×0.23 mm in the guinea pig model.

As indicated above, the insertion of a positioner into the cochlea has two mechanical effects: pushing the electrode into a modiolus hugging-position and causing a deeper insertion into the cochlea. The main purpose of this study was to observe the effect of lateral-to-medial displacement, rather than the effect of deeper electrode insertion. However, in vivo in humans, as well as in both modeled cochleae, the rotational position of the most basal electrode contact (No. 16) was negligibly changed by the positioner, allowing for a direct comparison of the results for this contact with and without a positioner. For more apical contacts, which are inserted considerably (up to half a turn) deeper, this is not a valid procedure, because it implies interference between the effects of the tapering of the scala tympani and the effects that result directly from the lateral-to-medial displacement of the electrode. Therefore, each comparison between situations with and without a positioner was carried out while looking at a fixed rotational position of the stimulated electrode (thereby changing the number of the stimulated electrode between situations).

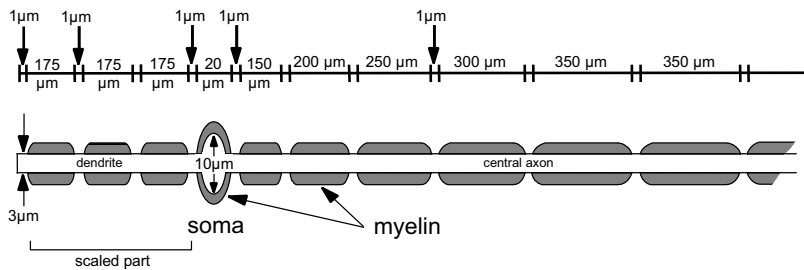


Figure 5.5: The morphology of the generalized Schwarz & Eikhof-Frijns auditory nerve fiber model as used in the calculations. The lengths of the three internodes in the so-called dendrite were scaled to adapt the fibers to the cochlea meshes.

5.2.3 Calculating the neural responses

The nonlinear generalized Swartz & Eikhof-Frijns model of primary auditory nerve fibers was used to simulate the response to time-varying potential fields in the cochlea. The model equations of this auditory nerve fiber model, which has nodal kinetics based on voltage clamp data in the rat (Schwarz and Eikhof,

1987), are described in detail elsewhere (Frijns et al., 1995) and are not reproduced here.

Figure 5.5 shows the morphology of the bipolar high spontaneous rate auditory fibers used in the calculations. These fibers, which were also used in our previous studies (Frijns et al., 1995; Frijns et al., 1996a; Frijns et al., 2000a; Briaire and Frijns, 2000b), consist of a peripheral and a modiolar axon with a diameter of 3 μm , interconnected by a cell body with a diameter of 10 μm . The gap width of the nodes of Ranvier is 1 μm . To accommodate the fibers to the cochlear meshes, we positioned the peripheral ending and the cell body of each fiber to their histologically correct positions and scaled the internodal lengths of the peripheral process accordingly.

5.3 Results

For all simulations presented here, we used cathodic-first symmetric biphasic current pulses (200 $\mu\text{s}/\text{phase}$) injected in a monopolar stimulation mode — i.e., against a far-field point current source — at different electrode contacts. The neural responses were plotted as I/O curves (Figs. 5.7 and 5.9), showing the fraction of all fibers that were excited as a function of stimulus level. By their nature, these I/O curves are closely related to the I/O curves calculated from electrically elicited whole nerve action potentials. The simulated I/O curves were computed on the basis of the underlying excitation profiles (Figs. 5.6 and 5.8, respectively), which show which fibers (ordered according to their rotational position Υ) are excited at each stimulus level. In these excitation profiles the part of the fiber (peripheral process, cell body or central axon) where the initial excitation takes place is indicated by gray shading. A narrow peak around the stimulated electrode in an excitation profile indicates that that mode of stimulation is selective. Such a selective stimulation is reflected in a relatively shallow slope of the I/O curve for stimulus levels immediately above threshold.

Figure 5.6 shows the excitation profiles computed for the Clarion HiFocus electrode without (GP lateral, A and C) and with (GP medial, B and D) positioner in the guinea pig cochlea. Figure 5.6^{A,B}, shows the computation for the most basal electrode (No. 16, $\Upsilon=0.4$), and Figure 5.6^{C,D}, shows the data for $\Upsilon=1.4$ turn (electrodes No. 1 and No. 5, respectively). The corresponding I/O curves are shown in Figure 5.7. In these figures it is readily seen that shifting the electrode from a conventional (lateral) to a modiolus-hugging position did not

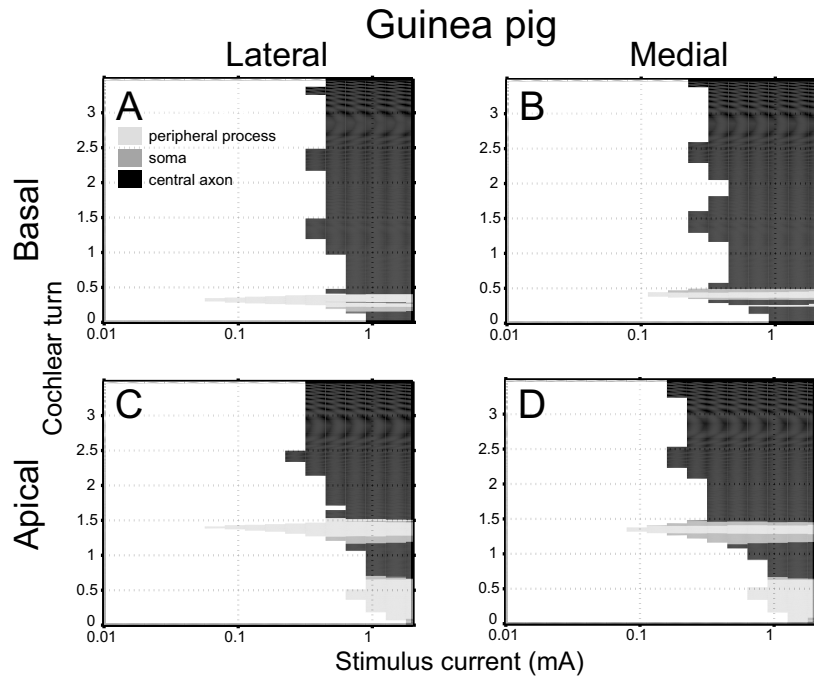


Figure 5.6: Excitation profiles for monopolar electrode configurations (cathodic-first biphasic current pulses, $200 \mu\text{s}/\text{phase}$) with the guinea pig equivalent of the Clarion HiFocus electrode in a lateral position (**A** and **C**) and with positioner (**B** and **D**). The location of the part of the nerve fiber where the initial excitation takes place is indicated by gray shading. **A** and **B** were computed for the most basal electrode contact (No. 16, $\Upsilon=0.4$) and **C** and **D** for the more apical contact at rotational position $\Upsilon=1.4$ (No. 1 and No. 5, respectively).

necessarily produce the desired reduction in threshold. On the contrary, for electrode No. 16 it even resulted in a considerable upward threshold shift. As can be seen by comparison of Figure 5.6^A and with Figure 5.6^B, this unexpected result is the consequence of the fact that the predicted site of excitation changes from the peripheral process (lateral position) to the cell body and modiolar part of the nerve fibers. This effect is less prominent for the apical electrodes, where the excitation threshold for the fibers at the same rotational position as the electrode is only marginally influenced by the lateral-to-medial shift. For both the apical and the basal electrodes, however, the modiolus hugging position leads to lower excitation thresholds for the fibers originating in more apical turns, which encode for lower frequencies in the physiologic situation. This so-called ectopic or cross-turn excitation occurs in the modiolus, where their central axons pass near the site of the stimulated electrode.

In humans, most excitation thresholds are higher (by a factor up to 10) as can be seen in the excitation profiles of Figure 5.8 and the corresponding I/O curves in Figure 5.9. This is not surprising, because the dimensions of the human cochlea are larger than those in the guinea pig counterpart. Especially for lateral electrode positions, this also leads to a somewhat larger range of stimulus levels before generalized excitation, as indicated by the steep part of the I/O curve, occurs. However, medializing the electrode with the positioner reveals a more striking difference between the human and animal model: With electrode No. 16 ($\Upsilon=0.2$, i.e., in the basal turn) in the human model, it reduces the excitation threshold for the fibers in the implanted turn by a factor of 4, whereas the threshold for cross-turn excitation is reduced by no more than a factor of 2 (Fig. 5.8^{A,B}). This means that in contrast to the guinea pig the lateral-to-medial displacement here reduces the amount of current needed to reach threshold and increases the dynamic range, while retaining the spatial selectivity. In the lateral position lower excitation thresholds are found for apical electrode No. 1 ($\Upsilon=1.0$) than for basal electrode No. 16 ($\Upsilon=0.2$) as a consequence of the smaller dimensions of the scala tympani. In the modiolus-hugging position, the threshold is further reduced, but with it the thresholds for fibers originating in the most apical turn are lowered as well. Unfortunately, this leads to a smaller range of stimulus levels before cross-turn excitation occurs. Thus, with respect to apical electrodes, the human situation is grossly comparable with the guinea pig equivalent.

Figure 5.10 gives the explanation for the different behavior in both species for basal and apical electrodes. It shows the potential distribution caused by a current of 1 mA injected into the cochlea through basal and apical electrodes in the monopolar mode in the GP medial and the human medial situations.

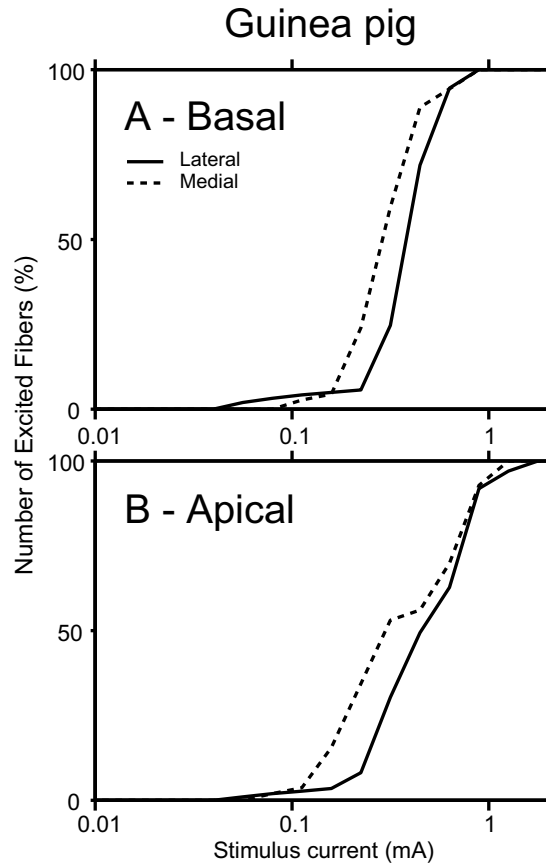


Figure 5.7: The effect of lateral-to-medial displacement in the guinea pig of the Clarion HiFocus electrode on threshold and slope of the I/O curve, which shows the fraction of the nerve fibers that is excited as a function of the stimulus level. **A**: Basal electrode contact (No. 16, $\Upsilon=0.4$), cathodic-first biphasic current pulses, $200 \mu\text{s}/\text{phase}$. **B**: As in **A** but now for the electrode contact at $\Upsilon=1.4$ (No. 1 in the lateral and No. 5 in the medial position).

For a correct interpretation of this figure, it is important to realize that not the absolute potential but the so-called activating function (Rattay, 1989) (roughly speaking, the [spatial] rate with which the potential gradient changes along the nerve fiber) is the main force leading to excitation of the nerve fibers. From Figure 5.10^A (GP medial situation, contact No. 16) it is clear that all fibers, regardless their site of origin, are exposed to fields with high gradient variations when they pass by the basal turn in the modiolus. The situation in Figure 5.10^C (human medial, contact No. 16) is fairly different: Fibers from the second turn pass through the outskirts of the potential field and follow almost the course of equipotential lines, whereas fibers from the apical region are even less likely to be stimulated. Comparison between Figure 5.10^B and Figure 5.10^D, showing the computations for apical electrodes, leads to a different analysis: For such apical electrode contacts, the implant sets up large potential gradients in the modiolus for both species, leading to a large likelihood of cross-turn stimulation for more apical turns. The fact that cross-turn stimulation is not an issue with regard to more basal turns in all species (Fig. 5.6^{C,D}; Fig. 5.8^{C,D}) is clarified further by Figure 5.10^{B,D}. This phenomenon requires direct stimulation of the dendritic part of the fibers in the turn immediately below the stimulated electrode. These fibers are relatively far away and are shielded from the electrode contact by the electrode carrier and — especially in the guinea pig — the insulating membranes surrounding the scala media.

5.4 Discussion and Conclusions

The main purpose of this modeling study was to obtain a better understanding of the circumstances under which modiolus-hugging scala tympani electrodes provide improvements over electrodes close to the lateral wall. The results suggest that the specific human cochlear anatomy, especially that of the basal turn, is a key factor in the potential success of approaching the modiolus as attempted with several modern electrode arrays (Gstoettner et al., 1999; Kuzma and Balkany, 1999; Aschendorff et al., 1999). The model predicts that the proximity of the electrode contacts to the excitable elements in the modiolus leads to reduced current thresholds while retaining a good dynamic range and spatial selectivity, at least for electrode contacts in the basal turn. To arrive at this conclusion, we introduced in this study a new volume conduction model of the human cochlea. Because the aim of this study did not allow ignoring the influence of the insulating electrode carrier, we included a detailed model of the Clarion HiFocus electrode array.

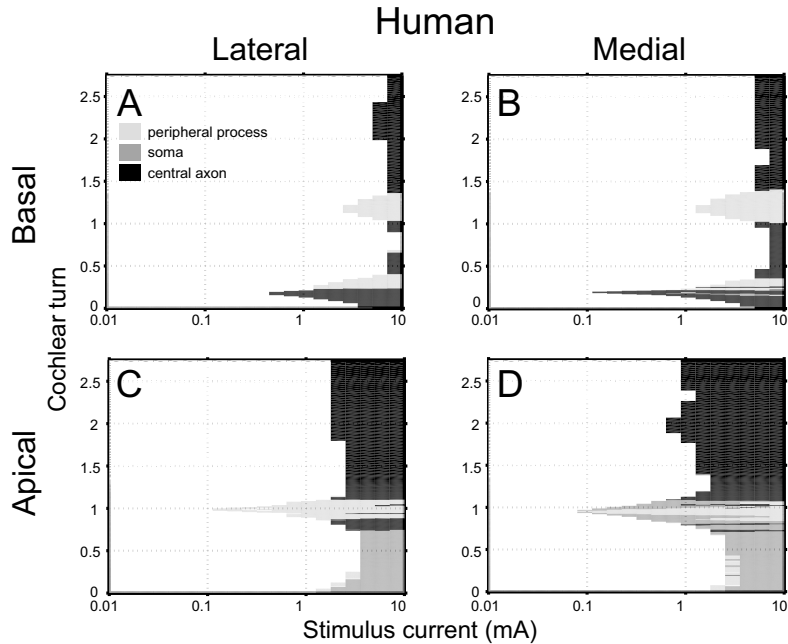


Figure 5.8: Excitation profiles for monopolar electrode configurations (cathodic-first biphasic current pulses, $200 \mu\text{s}/\text{phase}$) with the Clarion HiFocus electrode in a lateral position (**A** and **C**) and with the positioner (**B** and **D**) in the human cochlea. **A** and **B** were computed for the most basal electrode contact (No. 16, $\Upsilon=0.2$) and **C** and **D** for the more apical contact at rotational position $\Upsilon=1.0$ (No. 1 and No. 5, respectively).

The same electrode design (scaled down in size to fit the smaller cochlea) was tested in a model with the anatomy of the guinea pig cochlea, based on the previously validated (Frijns et al., 1995; Frijns et al., 1996a; Frijns et al., 2000a) numerical methods and parameters. This led to the somewhat paradoxical conclusion that approaching the modiolus does not necessarily lower the threshold level as it does in the human basal turn, whereas the dynamic range can be seriously reduced by the occurrence of cross-turn stimulation via the modiolus. The phenomenon of cross-turn stimulation is expected to lead to perceptual difficulties, because gradually increasing the stimulus level will suddenly lead to excitation of fibers that are physiologically associated

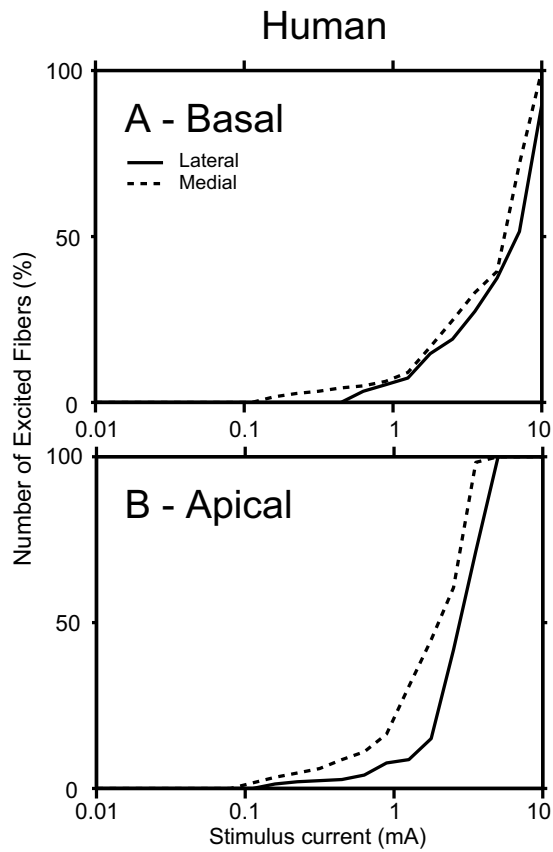


Figure 5.9: The effect of lateral to medial displacement in the human cochlea of the Clarion HiFocus electrode on threshold and slope of the I/O curve. **A:** Basal electrode contact (No. 16, $\Upsilon=0.2$), cathodic-first biphasic current pulses, $200 \mu\text{s}/\text{phase}$. **B:** As in **A** but now for the electrode contact at rotational position $\Upsilon=1.0$ (No. 1 in the lateral and No. 5 in the medial position).

with far lower frequencies. Such an effect has been reported in humans. Interestingly, that effect was more marked for wide bipolar stimulation than for monopolar stimulation (Cohen et al., 1996). As for the Clarion HiFocus electrode in humans, the fact that its apical electrode contacts perform better in a lateral position, while modiolus-hugging is better for the contacts in the basal turn, also has implications for safety: There is no advantage in pushing the positioner farther than one turn into the scala tympani, so one should avoid the risk of causing damage to the cochlear structures by exerting too much force on them when trying to obtain an unnecessarily deep insertion of the positioner. Future research with more sophisticated modes of stimulation than the monopolar mode we used may identify other ways to increase the spatial selectivity further, especially for more apical fibers.

An important body of cochlear implant research is formed by electrophysiologic studies in laboratory animals. Obviously, the underlying assumption is that the auditory system of the animals used in the studies is sufficiently comparable to the human equivalent to warrant a meaningful extrapolation of the results to the situation in deaf patients. In their recent study, Miller et al. (1999) found support for this hypothesis for psychophysical strength-duration functions. The strikingly different results between the human model and the guinea pig model pose some questions concerning the validity of this assumption for other aspects of electrical stimulation, especially because other species commonly used in auditory electrophysiology, like the cat, have many anatomical properties in common with the guinea pig. However, we also found that the guinea pig cochlea is a good model for the more apical parts of the human cochlea. Therefore, we conclude that one should always be cautious before interpreting animal experiments in terms of human applications. A computational model like the one used in this study, allowing manipulation of individual parameters while all the others are kept constant, may help to justify or reject such an extrapolation. In this study, the analysis of the potential distributions associated with the various electrode conditions in both species (Fig. 5.10) gave insight into the processes underlying results that were at first sight somewhat paradoxical.

As discussed in previous reports (Frijns et al., 1995; Frijns et al., 2000a), the exact value of the current thresholds predicted by the model is limited, because it is still a simplification of reality, dependent on many parameters that are not yet fully known. One of the known differences between the model and the in vivo situation in humans is the fact that the cell bodies in the spiral

ganglion are not myelinated (Arnold, 1987). Preliminary simulations, however, showed that this only slightly influences the threshold for situations without neuronal degeneration, although it has marked influence on spike timing. In spite of these limitations, the model is applicable to testing different electrode designs against one another under identical, fully controlled conditions. By contrast with animal experiments and clinical experiments in humans, one does not have to deal with interindividual variations or difficulties in manufacturing or implanting (miniaturized versions of) electrodes. For example, one of the main electroanatomical differences between the Clarion HiFocus electrode with positioner tested in this study and a new precurved intracochlear electrode with stylet from Cochlear Corp. (Melbourne, Australia) (Aschendorff et al., 1999) is the absence of a positioner lateral to the electrode in the latter case. The model allowed performing simulations with the Clarion HiFocus electrode in the medial position without the presence of the space-occupying positioner, thereby increasing the similarity with the precurved array with stylet. We found the same excitation thresholds and spread of excitation with increasing stimulus levels as with the positioner for all electrode contacts tested. In the human cochlea, the Silastic positioner appears to act as an insulator that shields the peripheral processes of the fibers one turn above the electrodes in the basal turn from direct excitation at higher stimulus levels, thereby increasing the dynamic range before ectopic stimulation occurs (Fig. 5.10^C).

We have also performed calculations with the precurved Clarion electrode array, which has ball contacts located below the dendrites and at the modiolar side of a tapered cylindrical carrier. Clinically, this electrode has been implanted with the same positioner as used with the Clarion HiFocus electrode (Kuzma and Balkany, 1999) in an attempt to take advantage of the modiolus-hugging effect. Although radiography revealed that the electrode was in the correct place, and a deeper insertion was obtained with the positioner (T. Balkany, personal communication), the effect on excitation thresholds was not unequivocal. This observation is in accordance with our simulation results, which show that the excitation thresholds are virtually unchanged, at least with the bipolar modes of stimulation used clinically. The main effect of the positioner is that less current is necessary to excite increasing numbers of nerve fibers. Clinical experience has shown that this should be interpreted not as a degradation of spatial selectivity but as a way to obtain a reasonable loudness growth with moderate current levels.

The main conclusion to be drawn from this study is that the specific anatomy of

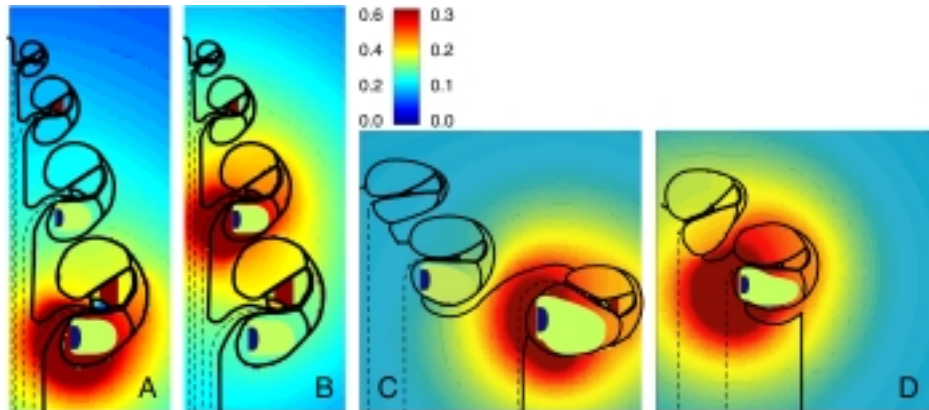


Figure 5.10: Potential plots for monopolar stimulation (1 mA) of the Clarion Hi-Focus electrode with positioner. The potential (in V) associated with the various gray levels is indicated by the color bar (the values to its left pertain to **A** and **B**; to the right, to **C** and **D**). The dashed lines illustrate the course of the primary auditory nerve fibers from the various turns. **A**: Basal electrode contact (No. 16, $\Upsilon=0.4$) in the guinea pig cochlea. **B**: Apical electrode contact (No. 5, $\Upsilon=1.4$) in the guinea pig cochlea. **C**: Basal electrode contact (No. 16, $\Upsilon=0.2$) in the human cochlea. **D**: Apical electrode contact (No. 5, $\Upsilon=1.0$) in the human cochlea.

the human cochlea has important beneficial implications for the clinical applicability of multichannel cochlear implants. The results shown in this study indicate that modiolus-hugging per se is not a universal remedy but is a promising method, to be tested in the basal turn with well-designed electrode arrays in humans rather than in animal models.

5.5 Acknowledgement

The authors thank Dr. F. Linthicum of the House Ear Institute for kindly providing the histologic cross-section used to construct the human mesh.